





Article

# [Fe( $\mu_2$ -OH) $_6$ ] $^{3-}$ Linked Fe $_3$ O Triads: Mössbauer Evidence for Trigonal $\mu_3$ -O $^{2-}$ or $\mu_3$ -OH $^-$ Groups in Bridged versus Unbridged Complexes

D. Nirosha T. De Silva<sup>1</sup>, Tyson N. Dais<sup>1,\*</sup> , Geoffrey B. Jameson<sup>1</sup> , Casey G. Davies<sup>2</sup>, Guy N. L. Jameson<sup>2,3</sup>  and Paul G. Plieger<sup>1,\*</sup> 

<sup>1</sup> School of Natural Sciences, Massey University, Private Bag 11 222, Palmerston North 4442, New Zealand

<sup>2</sup> Department of Chemistry, University of Otago, Dunedin 9016, New Zealand; casey.davies@otago.ac.nz (C.G.D.); guy.jameson@unimelb.edu.au (G.N.L.J.)

<sup>3</sup> Bio21 Molecular Sciences and Biotechnology Institute, The University of Melbourne, Parkville 3052, VIC, Australia

\* Correspondence: t.dais@massey.ac.nz (T.N.D.); p.g.plieger@massey.ac.nz (P.G.P.)

**Abstract:** The syntheses, coordination chemistry, and Mössbauer spectroscopy of hepta-iron(III) complexes using derivatised salicylaldoxime ligands from two categories; namely, ‘single-headed’ (H $_2$ L) and ‘double-headed’ (H $_4$ L) salicylaldoximes are described. All compounds presented here share a [Fe $_3$ - $\mu_3$ -O] core in which the iron(III) ions are  $\mu_3$ -hydroxo-bridged in the complex **C1** and  $\mu_3$ -oxo-bridged in **C2** and **C3**. Each compound consists of 2 × [Fe $_3$ - $\mu_3$ -O] triads that are linked via a central [Fe( $\mu_2$ -OH) $_6$ ] $^{3-}$  ion. In addition to the charge balance and microanalytical evidence, Mössbauer measurements support the fact that the triads in **C1** are  $\mu_3$ -OH bridged and are  $\mu_3$ -O bridged in **C2** and **C3**.

**Keywords:** Mössbauer; iron cluster; coordination chemistry



**Citation:** De Silva, D.N.T.; Dais, T.N.; Jameson, G.B.; Davies, C.G.; Jameson, G.N.L.; Plieger, P.G. [Fe( $\mu_2$ -OH) $_6$ ] $^{3-}$  Linked Fe $_3$ O Triads: Mössbauer Evidence for Trigonal  $\mu_3$ -O $^{2-}$  or  $\mu_3$ -OH $^-$  Groups in Bridged versus Unbridged Complexes. *Molecules* **2024**, *29*, 3218. <https://doi.org/10.3390/molecules29133218>

Academic Editors: Juan Nicolás-Gutiérrez and Miquel Barceló-Oliver

Received: 17 June 2024

Revised: 2 July 2024

Accepted: 4 July 2024

Published: 7 July 2024



**Copyright:** © 2024 by the authors. Licensee MDPI, Basel, Switzerland. This article is an open access article distributed under the terms and conditions of the Creative Commons Attribution (CC BY) license (<https://creativecommons.org/licenses/by/4.0/>).

## 1. Introduction

Polynuclear iron complexes have attracted interest due to their importance as both biological [1–6] and magnetic materials [7–11]. Herein, we report on the syntheses and coordination chemistry of three heptanuclear iron complexes built with derivatised salicylaldoximato ligands. The hepta-Fe(III) complexes presented here all share the common building block [Fe $_3$ O], in which Fe(III) ions are bridged by oximato- and oxo/hydroxo- groups. Salicylaldoximes and derivatised salicylaldoximes are well known to form multinuclear species that contain these triangular metal rings with three-fold symmetry (Figure 1) [12,13]. Study of this class of iron clusters has been fueled by the presence of analogous iron units observed in biologically important metalloproteins [2,14–22] and also as analogues of magnetically interesting manganese complexes [23]. The first iron–salicylaldoximato cluster reported was a tetra-iron species, [Fe $_4$ (saoH) $_4$ (sao) $_4$ ] [24] of which the chemistry was later extended by Raptopoulou et al. [13] to produce a tri-iron(III) compound with a [Fe $_3$ O] $^{7+}$  core, coordinated by five benzoate ions and a salicylaldoximato di-anion.

A similar tri-iron(III) compound with the same core formed with six benzoate ions, an azido anion, and two bound ethanol molecules was reported by Boudalis et al. [12]. Recently, there have been several more examples reported for tri-, hexa-, and hepta-iron(III) salicylaldoximato/derivatised salicylaldoximato complexes containing the [Fe $_3$ O] $^{7+/8+}$  core [23,25–28]. The first polynuclear copper complex with a linked derivatised salicylaldoximato ligand, *N,N'*-dimethyl-*N,N'*-hexamethylenebis(5-*tert*-butyl-2-hydroxy-3-hydroxyiminomethyl)benzylamine (H $_4$ L), was reported by Plieger et al. in 2009 [29]. This helical hexa-copper complex motivated us towards the synthesis of analogous iron(III) compounds with the same class of ligands [30]. However, in 2012, Brechin et al. [23] reported an

iron(III) analogue of this hexa-copper complex using  $H_4L$  [29]. This was the hepta-iron(III) cluster,  $[Fe_7(\mu_3-O)_2(\mu_2-OH)_6(H_2L-2H)_3(pyr)_6] \cdot 5BF_4 \cdot 6H_2O \cdot 14MeOH, 1 \cdot 2BF_4 \cdot 6H_2O \cdot 14MeOH$ , consisting of two triangles of  $[Fe_3O]^{7+}$ , which are linked via a central  $[Fe(OH)_6]^{3-}$  ion and three helical ( $H_4L-2H$ ) ligands.

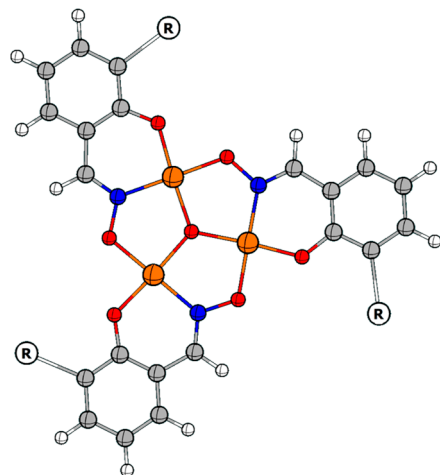


**Figure 1.** A schematic of the planar  $[M_3O(oximato)_3]^{+/++}$  moiety with three-fold symmetry. C = grey, M = orange, N = blue, O = red, and R = the rest of the ligand.

Salicylaldoxime-based ligands are of particular interest due to the ease in derivatizing the aromatic ring and the inherent ability of the oximato moiety to coordinate multiple metal centres in close proximity. We herein report the syntheses and structures of three analogues (**C1–C3**) of the hepta-iron(III) complex **1** and use Mössbauer spectroscopy to evidence unexpected speciation of the central  $\mu_3$ -oxygen atom.

## 2. Results

### 2.1. Discussion of the Crystal Structure of the $Fe_7$ Complex of a ‘Single-Headed’ Derivatised Salicylaldoxime (**C1**)

The first hepta-iron(III) compound, **C1**, was synthesised using a simple derivatised salicylaldoxime ligand,  $H_2L1$  (2-hydroxy-5-*tert*-butyl-3-(*N*-piperidinylmethyl)benzaldehyde oxime) (Figure 2) [31–33]. Slow evaporation of the filtrate from the 1:1 reaction mixture of  $Fe(BF_4)_2 \cdot 6H_2O$  and the ligand,  $H_2L1$ , in a methanol-pyridine solution led to the formation of dark maroon rhombic-shaped crystals of the hepta-iron(III) cluster,  $[Fe_7(\mu_3-OH)_2(\mu_2-OH)_6(H_2L1-2H)_5(H_2L1-H)(pyr)_6] \cdot (BF_4)_2 \cdot (H_2O)_6 \cdot (pyr)_3$  (**C1**· $2BF_4 \cdot 8H_2O \cdot 2pyr$ ) which crystallised in the  $R\bar{3}$  space group.

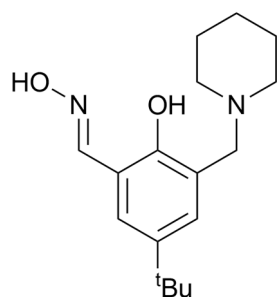


**Figure 2.** The chemical structure of the non-linked/single headed salicylaldoxime ligand,  $H_2L1$ , utilised for the synthesis of the  $Fe_7$  complex **C1**.

One sixth of the complex **C1** represents the asymmetric unit, and the full complex is generated by an  $S_6 - \bar{3}$  improper rotation. There are six molecules of the ligand  $H_2L1$  in the di-anionic form,  $H_2L1-2H$ , in the complex, which are directly connected to six iron atoms

( $6 \times \mu_3\text{-Fe}_2$ ) that form two metal triads of  $[\text{Fe}^{\text{III}}_3(\mu_3\text{-OH})]^{8+}$ , which are exactly parallel to each other (Figure 3). The central oxygen of the triad is formulated as a hydroxo species based on Mössbauer spectroscopy (see below). These triads are linked via six hydroxo groups that provide the coordination sphere to a seventh iron atom (Fe1), which sits in the middle of the complex as an anion  $[\text{Fe}(\mu_2\text{-OH})_6]^{3-}$  and is located 3.118 Å from the metal triads (the distance between the metal planes is 6.237 Å). Each triangle consists of three doubly deprotonated ligands ( $\text{H}_2\text{L1-2H}$ ), three iron(III) bound to a  $\mu_3\text{-OH}$  and three capping pyridine molecules (pyr). Thus, the positive charge (+21) provided by the seven  $\text{Fe}^{\text{III}}$  is overbalanced by  $-12$  from the six ligands,  $-8$  from hydroxo groups [ $2 \times (\mu_3\text{-OH}) + 6 \times (\mu_2\text{-OH})$ ], and  $-2$  from  $2 \times \text{BF}_4^-$  ions present within the lattice. Charge neutrality is achieved by a single proton distributed randomly over the 6 piperidinyl groups of the salicylaldoximato ligand.

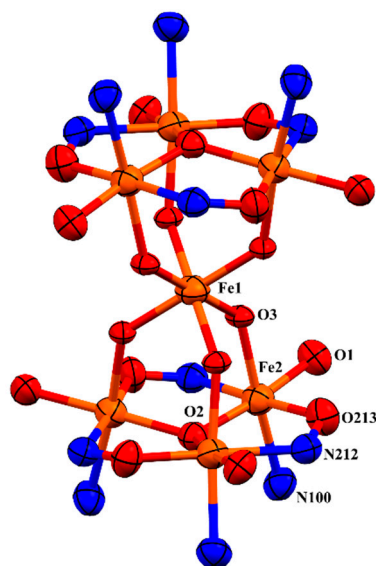


**Figure 3.** The core of complex **C1**. Fe = orange, N = blue, O = red. Thermal ellipsoids shown at 70% probability level.

Each iron atom of the complex is hexa-coordinated and sits in an approximately octahedral geometry. Equatorial sites around each iron atom of the triads (Fe2) are occupied by a phenolato oxygen (O1) atom and an oximato nitrogen (N212) atom from one ligand and an oximato oxygen (O213) atom from a neighbouring ligand and a central oxygen atom ( $\mu_3\text{-O}$ ). A pyridine group (N100) and a hydroxo group ( $\mu_2\text{-OH}$ ) are axially coordinated to each iron atom (Fe2) of the triangles. The iron centres of each metal triangle are held together by three N-O groups from the ligands resulting in a bridge between two neighbouring iron atoms. The bridging sequence is as Fe-O-N-Fe on both metal triangles. The central oxygen atom,  $\mu_3\text{-O}$ , of the metal triangle is displaced out of the metal planes by 0.314(6) Å away from the centre of the complex. The consequence is that the axial pyridyl groups tilt slightly away from each other, relieving steric strain. The Fe atom from  $[\text{Fe}(\mu_2\text{-OH})_6]^{3-}$  sits in an almost perfect octahedral coordination environment, as a consequence of sitting on the  $S_6\text{-}\bar{3}$  axis. The hourglass-like metallic core of **C1** is illustrated in Figure 3, and selected bond lengths and angles around Fe1 and Fe2 are shown in Table 1.

Additionally, water and pyridine molecules exist within the lattice. The hydroxo groups ( $\mu_2\text{-OH}$ ) form strong hydrogen bonds (1.880 (10) Å) with water molecules and also moderately strong hydrogen bonds with neighbouring phenolato oxygen atoms, O1 (2.559 (6) Å) [34]. The composition of the crystal structure of this complex is confirmed by microanalytical data, charge balance, and Mössbauer.

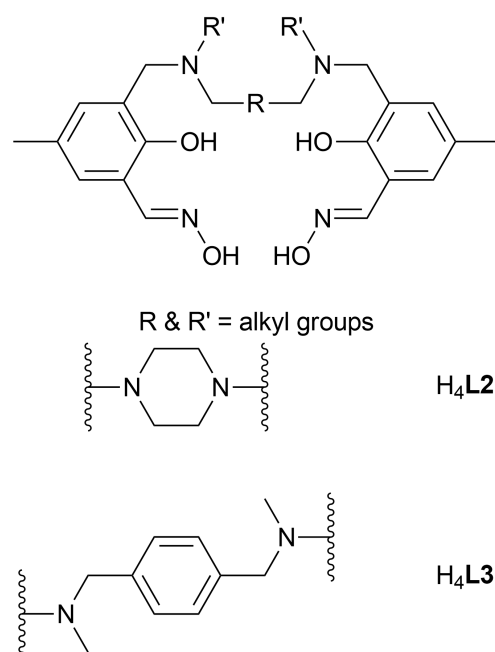
**Table 1.** Selected structural parameters for C1·2BF<sub>4</sub>·8H<sub>2</sub>O·2pyr.

Atoms	Length (Å)	Atoms	Length (Å)
Fe2–O2	1.9287 (11)	Fe2–N100	2.208 (4)
Fe2–O213	1.959 (3)	Fe2–O3	2.043 (3)
Fe2–O1	1.939 (3)	Fe1–O3	1.920 (2)
Fe2–N212	2.124 (3)	O213–N212	1.378 (6)
Atoms	Angle (°)	Atoms	Angle (°)
N100–Fe2–O2	94.9 (2)	O1–Fe2–O2	172.6 (2)
N100–Fe2–O213	90.1 (2)	O213–Fe2–N212	176.5 (2)
N100–Fe2–O1	88.1 (2)	O1–Fe2–O213	91.5 (2)
N100–Fe2–N212	90.0 (2)	O213–Fe2–O2	95.2 (2)
O3–Fe2–O1	87.0 (2)	O2–Fe2–N212	88.3 (2)
O3–Fe2–O2	89.7 (2)	N212–Fe2–O1	85.1 (2)
O3–Fe2–N212	87.2 (2)	Fe1–O3–Fe2	133.8 (2)
Fe2–O2–Fe2 *	117.4 (2)	O3–Fe1–O3 *	89.8 (2)
N100–Fe2–O3	174.5 (2)		

\* Generated by  $S_6\bar{3}$  symmetry.

## 2.2. Discussion of the Crystal Structures of Fe<sub>7</sub> Complexes of Linked/'Double-Headed' Derivatised Salicylaldoximes

The complexes, **C2** and **C3** are double-headed,  $\mu_3$ -oxo-bridged hepta-iron(III) compounds produced in the form of dark red rhombic crystals. Both were obtained by slow evaporation of filtered reaction mixtures of the iron salt Fe(BF<sub>4</sub>)<sub>2</sub>·6H<sub>2</sub>O and the corresponding ligand (H<sub>4</sub>L<sub>2</sub> and H<sub>4</sub>L<sub>3</sub>, respectively) in the presence of NaPF<sub>6</sub> at a 1:2:2 ratio in a methanol-pyridine solution. These complexes are analogues of **C1**. Despite the different amine linkers present in the ligands (Figure 4) and the additional non-coordinated species present within the lattices, **C2** and **C3** are structurally very similar. Each of these clusters contains two approximately parallel oximato- and oxo-bridged metal triangles connected to a central Fe(III) atom via six hydroxo groups. X-ray crystal structures of the hepta-iron(III) clusters, **C2** and **C3**, are described in this section. Selected structural parameters for these complexes can be found in Table 2.

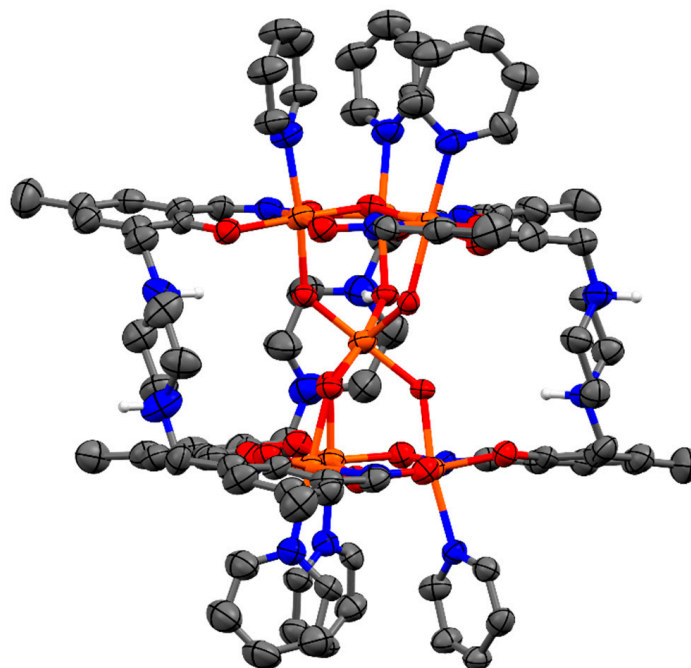


**Figure 4.** The structural representative of the linked/'double-headed' salicylaldoxime ligand (top) and the diamine linkers of the ligands H<sub>4</sub>L<sub>2</sub>, H<sub>4</sub>L<sub>3</sub> (bottom).

**Table 2.** Selected structural parameters for **C2** and **C3**.

	<b>C2</b>	<b>C3</b>
<b>Atoms</b>	<b>Length (Å)</b>	<b>Length (Å)</b>
Fe <sub>tri</sub> -μ <sub>3</sub> O	1.881 (7)–1.952 (7)	1.913 (4)–1.936 (3)
Fe <sub>tri</sub> -μ <sub>2</sub> OH	1.997 (6)–2.034 (6)	2.036 (3)–2.045 (3)
Fe <sub>mid</sub> -μ <sub>2</sub> OH	1.911 (6)–1.969 (6)	1.964 (3)–1.972 (3)
Fe <sub>plane</sub> -μ <sub>3</sub> O	0.338–0.376	0.330
Fe <sub>mid</sub> -μ <sub>3</sub> O	3.447 (7)–3.491 (8)	3.512 (4)
μ <sub>3</sub> O-μ <sub>3</sub> O	6.938 (10)	7.024 (4)
<b>Atoms</b>	<b>Angle (°)</b>	<b>Angle (°)</b>
Fe <sub>tri</sub> -μ <sub>3</sub> O-Fe <sub>tri</sub>	114.6 (3)–119.2 (4)	116.2 (2)–118.0 (2)
Fe <sub>tri</sub> -μ <sub>2</sub> OH-Fe <sub>mid</sub>	131.6 (4)–136.3 (4)	134.6 (6)–135.3 (6)
μ <sub>3</sub> O-Fe <sub>mid</sub> -μ <sub>3</sub> O	178.2 (2)	180

Of particular note are the Fe-μ<sub>3</sub>-oxo bond lengths and displacements of the triply-bridging oxygen atom from the planes of the Fe<sub>3</sub> moiety, which are not significantly different for the [Fe<sub>3</sub><sup>III</sup>-μ<sub>3</sub>-OH]<sup>8+</sup> moiety of **C1**, and the [Fe<sub>3</sub><sup>III</sup>-μ<sub>3</sub>-O]<sup>7+</sup> of **1** and **C2** and **C3**. Therefore, there is no crystallographic evidence to distinguish μ<sub>3</sub>-O atoms being hydroxo in **C1** from their being oxo in **C2** and **C3**. In contrast to the [Fe<sub>3</sub><sup>III</sup>-μ<sub>3</sub>-OH]<sup>8+</sup> of **C1**, the metal triads are formulated as [Fe<sub>3</sub><sup>III</sup>-μ<sub>3</sub>-O]<sup>7+</sup> on the basis of Mössbauer spectroscopy. In **C2**, the oximate bridging sequence on the upper triangle is -N-O-, whereas it is -O-N- on the lower triangle. On the other hand, the same oximate bridging sequence occurs on both triangles of **C3**. As the ligands utilised for **C2** and **C3** are flexible linked salicylaldoximes containing salicylaldoxime units on either side, only three ligand molecules are required to form a hepta-iron(III) complex, unlike those used for **C1**. Three of these ‘salicylaldoxime heads’ from three ligand molecules form a lower triangle and the other three ‘heads’ form an upper triangle (Figure 1). Due to the flexibility of the di-amine linker between the salicylaldoxime ‘heads’, these complexes take a twisted helical shape (Figure 5).

**Figure 5.** X-ray crystal structure of complex **C2**. Anions and non-interacting H atoms omitted for clarity. Fe = orange, N = blue, O = red; thermal ellipsoids shown at 30% probability level.

### 2.3. Mössbauer Results and Discussion

$^{57}\text{Fe}$  Mössbauer measurements were performed on complexes **C1–C3** at low and room temperature. Integral fits of the transmission were carried out for the data obtained at room temperature. The parameters for each of the samples are listed in Table 3.

**Table 3.** Room temperature  $^{57}\text{Fe}$  Mössbauer fitting parameters for **C1–C3** ( $\delta$  = isomer shift,  $\Delta E_Q$  = quadrupole splitting,  $\Gamma$  = half height line width,  $I$  = intensity).

Complex	$\delta$ (mm/s)	$\Delta E_Q$ (mm/s)	$\Gamma_L$ (mm/s)	$\Gamma_R$ (mm/s)	$I$ (%)
<b>C1</b>	0.41	0.86	0.37	0.37	77.8
	0.40	0.50	0.21	0.21	28.9
<b>C2</b>	0.40	1.50	0.35	0.35	70
	0.40	0.55	$0.35 \pm 0.15$	$0.35 \pm 0.15$	30
<b>C3</b>	0.40	1.55	0.30	0.30	75
	0.35	0.45	0.35	0.35	26

The spectra that were recorded at 293 K illustrate two distinctive fitting lines (red and blue) (Figures 6–8). These two lines can be unambiguously attributed to the two different iron environments present in each complex. The intensity of the blue peaks on the Mössbauer spectra of these complexes is much higher than that of the red peaks. The intensity ratio between the two iron species of each hepta-iron(III) compound was observed to be approximately 7:3, near enough to the expected value of 6:1 given by the crystallographic results, given that the central Fe atom is very tightly constrained relative to the iron triads. The isomer shift values of these complexes indicate the +3 oxidation state and high-spin state of the iron sites [35], and these numbers do not differ significantly among complexes **C1–C3** at 293 K. The quadrupole splitting value for **C1** ( $0.50 \text{ mm}^{-1}$  and  $0.87 \text{ mm}^{-1}$ ), on the other hand, is significantly different from the values obtained for **C2** and **C3** ( $0.45\text{--}0.55 \text{ mm}^{-1}$  and  $1.50\text{--}1.55 \text{ mm}^{-1}$ ) (see Table 3). The large quadrupole splitting (and relative intensity compared to the other doublet) is consistent with  $\mu_3$ -oxo groups for **C2** and **C3**. The smaller quadrupole splitting of the doublets of weaker intensity for **C2** and **C3** and the pair of quadrupole doublets for **C1** are consistent with  $\mu_2$ -hydroxo groups and for **C1** the  $\mu_3$ -hydroxo groups.

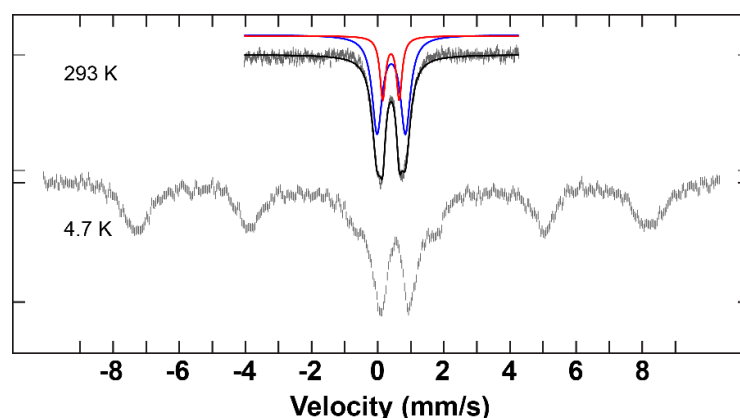


**Figure 6.**  $^{57}\text{Fe}$  Mössbauer spectra of the complex **C1** at high and low temperature and are overlaid with corresponding fits using the parameters given in Table 3 at high temperature.

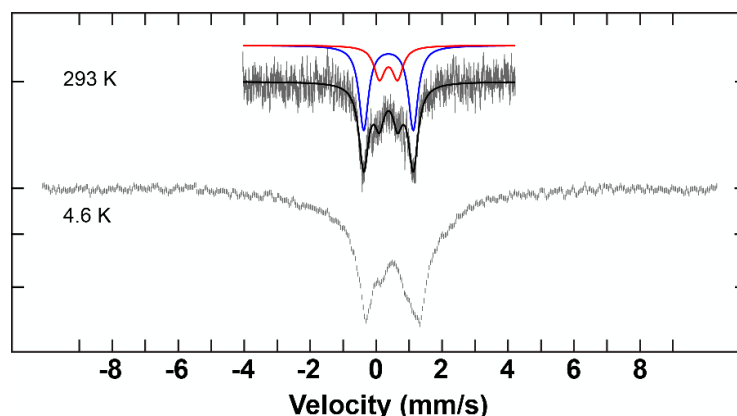


**Figure 7.**  $^{57}\text{Fe}$  Mössbauer spectra of the complex **C2** at high and low temperature and are overlaid with corresponding fits using the parameters given in Table 3 at high temperature.

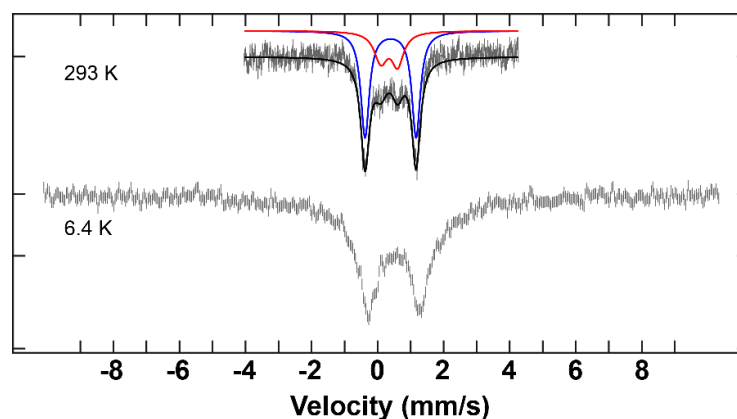


**Figure 8.**  $^{57}\text{Fe}$  Mössbauer spectra of the complex **C3** at high and low temperature and are overlaid with corresponding fits using the parameters given in Table 3 at high temperature.

### 3. Materials and Methods

All reactions were performed under aerobic conditions using chemicals and solvents as received, unless otherwise stated.  $^1\text{H}$  and  $^{13}\text{C}$  NMR spectra were recorded on a Bruker Avance 500 MHz spectrometer (Bruker, Billerica, MA, USA);  $\delta$  values are relative to TMS or the corresponding solvent. Mass spectra were obtained using a Micromass ZMD 400 electrospray spectrometer (Waters Corporation, Millford, MS, USA). IR spectra were recorded on a Nicolet 5700 FT-IR spectrometer from Thermo Electron Corporation (Thermo Electron Scientific Instruments Corp., Madison, WI, USA) using an ATR sampling accessory. Elemental analyses were determined by the Campbell Microanalytical Laboratory at the University of Otago.

#### 3.1. Synthesis of Ligands $\text{H}_4\text{L2}$ and $\text{H}_4\text{L3}$

The starting material of the multi-step ligand synthesis, 5-methylsalicylaldehyde, was synthesised as described in the literature [31]. The preparation of 3-(bromomethyl)-2-hydroxy-5-methylbenzaldehyde (**1**) and precursors **L2a** and **L3a** were carried out by the procedure of Tasker and Schröder [36]. The preparation of  $N,N'$ -dimethyl-*p*-xylenediamine (**2**), and the oximations were carried out according to the procedure by Plieger et al. [32] The ligand  $\text{H}_2\text{L1}$  was synthesised using the protocols in Tasker et al. [33] and Plieger et al. [37].

##### 3.1.1. **L2a** (Precursor for $\text{H}_4\text{L2}$ ): 3,3'-[1,4-Piperazinediylbis(methylene)]bis [2-hydroxy-5-methylbenzaldehyde]

Solutions of **1** (1.27 g, 5.54 mmol) and piperazine (0.242 g, 2.77 mmol), each in dry  $\text{CH}_2\text{Cl}_2$  (15 mL), were simultaneously added to a stirred solution of  $\text{Et}_3\text{N}$  (1.11 g, 11.0 mmol)

in dry  $\text{CH}_2\text{Cl}_2$  (20 mL). The resulting yellow solution was stirred for 24 h at room temperature (RT). The solution was washed with water ( $3 \times 70$  mL) and the organic phase dried over anhydrous  $\text{Na}_2\text{SO}_4$ . Removal of the solvent afforded a brown solid, which was purified by adding ethanol to a concentrated solution of the compound in  $\text{CHCl}_3$  affording a pale brown powder, which was dried in vacuo. Yield (0.90 g, 85%). MP 221–222 °C.  $\nu_{\text{max}}/\text{cm}^{-1}$  1679 (s). Found: C, 68.14; H, 6.74; N, 7.26. Calc for  $\text{C}_{22}\text{H}_{26}\text{N}_2\text{O}_4 \cdot 0.3\text{C}_2\text{H}_5\text{OH}$ : C, 68.44; H, 7.09; N, 7.04.  $^1\text{H}$  NMR (500 MHz;  $\text{CDCl}_3$ )  $\delta$ : 2.29 (s, 6H), 2.66 (br, 8H), 3.70 (s, 4H), 7.17 (d,  $J = 1.75$  Hz, 2H), 7.41 (d,  $J = 1.61$  Hz, 2H), 10.21 (s, 2H) ppm.  $^{13}\text{C}$  NMR (125 MHz;  $\text{CDCl}_3$ )  $\delta$ : 20.2, 52.4, 58.5, 122.0, 123.5, 128.4, 129.5, 137.0, 158.8, 192.6 ppm.  $m/z$  (ESI) 383  $[\text{M} + \text{H}]^+$ .

### 3.1.2. $\text{H}_4\text{L}_2$ : 3,3'-[1,4-Piperazinediylbis(methylene)]bis[2-hydroxy-5-methylbenzaldehyde oxime]

A solution of hydroxylamine hydrochloride (0.400 g, 5.76 mmol) in dry ethanol (60 mL) was neutralised with potassium hydroxide (0.324 g, 5.76 mmol) in dry ethanol (60 mL). The resulting white precipitate was removed, and the filtrate was added to a solution of **L2a** (0.727 g, 1.90 mmol) in 5 mL chloroform and 95 mL dry ethanol over 30 min. The pale yellow solution was stirred for a further 24 h at RT, during which time a pale yellow precipitate was formed. The precipitate was filtered, and the remaining solvent was removed under reduced pressure. The combined pale yellow residues were then washed with cold chloroform ( $3 \times 30$  mL) and dried in vacuo. Yield (0.321 g, 41%). MP 245–246 °C.  $\nu_{\text{max}}/\text{cm}^{-1}$  1625 (s), 1470 (s), 1136 (s), 822 (s). Found: C, 63.59; H, 6.84; N, 13.58. Calc for  $\text{C}_{22}\text{H}_{28}\text{N}_4\text{O}_4 \cdot 0.2\text{C}_2\text{H}_5\text{OH}$ : C, 63.80; H, 6.98; N, 13.29.  $^1\text{H}$  NMR (500 MHz;  $d_6$ -DMSO)  $\delta$ : 2.19 (s, 6H), 3.59 (s, 8H), 3.62 (s, 4H), 6.96 (d,  $J = 1.92$  Hz, 2H), 7.23 (d,  $J = 1.74$  Hz, 2H), 8.27 (s, 2H) ppm.  $^{13}\text{C}$  NMR (125 MHz;  $d_6$ -DMSO)  $\delta$ : 20.5, 52.4, 58.4, 118.5, 123.2, 126.5, 127.8, 131.6, 146.9, 153.6 ppm.  $m/z$  (ESI) 413  $[\text{M} + \text{H}]^+$ .

### 3.1.3. **L3a** (Precursor for $\text{H}_4\text{L}_3$ ):

#### 3,3'-[1,4-Phenylenebis[methylene(methylimino)methylene]]bis[2-hydroxy-5-methylbenzaldehyde]

Solutions of **1** (1.27 g, 5.54 mmol) and **2** (0.461 g, 2.77 mmol), each in dry  $\text{CH}_2\text{Cl}_2$  (15 mL), were simultaneously added to a stirred solution of  $\text{Et}_3\text{N}$  (1.11 g, 11.0 mmol) in dry  $\text{CH}_2\text{Cl}_2$  (20 mL). The yellow solution was stirred for 24 h at RT. The solution was washed with water ( $3 \times 70$  mL), and the organic phase dried over anhydrous  $\text{Na}_2\text{SO}_4$ . Removal of the solvent afforded a pale yellow solid, which was recrystallised by adding ethanol to a concentrated solution of the compound in  $\text{CHCl}_3$  affording yellow crystals, which were dried in vacuo. Yield (1.16 g, 90%). MP 152–155 °C.  $\nu_{\text{max}}/\text{cm}^{-1}$  1678 (s), 3449 (br), 828 (s). Found: C, 72.60; H, 6.87; N, 6.03. Calc for  $\text{C}_{28}\text{H}_{32}\text{N}_2\text{O}_4$ : C, 73.02; H, 7.00; N, 6.08.  $^1\text{H}$  NMR (500 MHz;  $\text{CDCl}_3$ )  $\delta$ : 2.28 (s, 6H), 2.30 (s, 8H), 3.63 (s, 4H), 3.73 (s, 4H), 7.19 (d,  $J = 1.79$  Hz, 2H), 7.34 (s, 4H), 7.44 (d,  $J = 1.57$  Hz, 2H), 10.31 (s, 2H) ppm.  $^{13}\text{C}$  NMR (125 MHz;  $\text{CDCl}_3$ )  $\delta$ : 20.3, 41.5, 58.5, 58.5, 61.4, 122.3, 124.2, 128.3, 128.7, 129.4, 136.5, 136.6, 159.1, 192.1 ppm.  $m/z$  (ESI) 461  $[\text{M} + \text{H}]^+$ .

### 3.1.4. $\text{H}_4\text{L}_3$ : 3,3'-[1,4-Phenylenebis[methylene(methylimino)methylene]]bis[2-hydroxy-5-methylbenzaldehyde oxime]

A solution of hydroxylamine hydrochloride (0.377 g, 5.43 mmol) in dry ethanol (60 mL) was neutralised with potassium hydroxide (0.323 g, 5.76 mmol) in dry ethanol (60 mL). The resulting white precipitate was removed, and the filtrate was added to a solution of **L3a** (1.00 g, 2.17 mmol) in 5 mL chloroform and 95 mL dry ethanol over 30 min. The pale yellow solution was stirred for a further 48 h at RT, after which time a pale yellow precipitate was obtained. The combined residues were filtered, washed with cold chloroform ( $3 \times 30$  mL) followed by cold ethanol ( $3 \times 30$  mL), and dried in vacuo. Yield (0.978 g, 92%). MP 203–204 °C.  $\nu_{\text{max}}/\text{cm}^{-1}$  1610 (m), 2955 (m), 1469 (vs), 1285 (s), 1020 (m). Found: C, 67.01; H, 6.96; N, 10.89. Calc for  $\text{C}_{28}\text{H}_{34}\text{N}_4\text{O}_4 \cdot 0.5\text{C}_2\text{H}_5\text{OH}$ : C, 67.81; H, 7.26; N, 10.91.  $^1\text{H}$  NMR (500 MHz;  $d_6$ -DMSO)  $\delta$ : 2.12 (s, 6H), 2.21 (s, 6H), 3.58 (s, 4H), 3.66 (s, 4H), 7.01 (d,  $J = 1.64$  Hz,



2H), 7.24 (d,  $J = 1.80$  Hz, 2H), 8.28 (s, 2H) ppm.  $^{13}\text{C}$  NMR (125 MHz;  $d_6$ -DMSO): 20.5, 41.3, 58.1, 60.7, 118.5, 123.9, 126.3, 127.9, 129.5, 131.3, 137.1, 146.9, 153.6 ppm.  $m/z$  (ESI) 491  $[\text{M} + \text{H}]^+$ .

### 3.2. Synthesis of Metal Complexes C1–C3

#### 3.2.1. $[\text{Fe}_7(\mu_3\text{-OH})_2(\mu_2\text{-OH})_6(\text{H}_2\text{L1-2H})_5(\text{H}_2\text{L1-H})_1(\text{pyr})_6] \cdot (\text{BF}_4)_2 \cdot (\text{H}_2\text{O})_8 (\text{pyr})_2$ (C1·2BF<sub>4</sub>·8H<sub>2</sub>O·2pyr)

To the ligand H<sub>2</sub>L1 (0.145 g, 0.50 mmol), dissolved in MeOH (12.5 mL), was added Fe(BF<sub>4</sub>)<sub>2</sub>·6H<sub>2</sub>O (0.169 g, 0.50 mmol) in MeOH (12.5 mL). After full dissolution, NaPF<sub>6</sub> (0.167 g, 1.00 mmol) and pyridine (2 mL) were added to the maroon-coloured solution. The mixture was stirred for 3 h and filtered, and the filtrate was left to evaporate slowly. X-ray quality crystals were produced after 2 weeks (CCDC 2331487). Yield (0.180 g, 67%). Found: C, 52.63; H, 6.35; N, 8.58. Calc for C<sub>132</sub>H<sub>183</sub>Fe<sub>7</sub>N<sub>18</sub>O<sub>20</sub>·2BF<sub>4</sub>·6H<sub>2</sub>O: C, 52.59; H, 6.52; N, 8.36.  $\bar{\nu}_{\text{max}}/\text{cm}^{-1}$  3388(br), 2967, 2370, 1605, 1550, 1459, 1084, 1040, 839, 732, 534, 437.

#### 3.2.2. $[\text{Fe}_7\text{O}_2(\text{H}_4\text{L2-2H})_3(\text{OH})_6(\text{pyr})_6] \cdot (\text{BF}_4)_4 \cdot (\text{H}_2\text{O})_7 \cdot \text{PF}_6 \cdot (\text{pyr})_2$ (C2·4BF<sub>4</sub>·7H<sub>2</sub>O·PF<sub>6</sub>·2pyr)

To the ligand H<sub>4</sub>L2 (0.206 g, 0.50 mmol), suspended in MeOH (12.5 mL), was added Fe(BF<sub>4</sub>)<sub>2</sub>·6H<sub>2</sub>O (0.348 g, 1.00 mmol) dissolved in MeOH (12.5 mL). After full dissolution, NaPF<sub>6</sub> (0.167 g, 1.00 mmol) and pyridine (2 mL) were added to the maroon-coloured solution. The solution was stirred for 3 h and filtered, and the filtrate was left to evaporate slowly. X-ray quality crystals were produced after 2 weeks (CCDC 2331488). Yield (0.200 g, 47%). Found: C, 40.24; H, 4.44; N, 8.84. Calc for C<sub>96</sub>H<sub>114</sub>Fe<sub>7</sub>N<sub>18</sub>O<sub>20</sub>·4BF<sub>4</sub><sup>−</sup>·7H<sub>2</sub>O·PF<sub>6</sub><sup>−</sup>: C, 40.47; H, 4.53; N, 8.85.  $\nu_{\text{max}}/\text{cm}^{-1}$  3412(br), 1724, 1703, 1613, 1552, 1463, 1307, 1084, 1034, 825, 757, 483, 434.

#### 3.2.3. $[\text{Fe}_7\text{O}_2(\text{H}_4\text{L3-2H})_2(\text{H}_4\text{L3-3H})(\text{OH})_6(\text{pyr})_6] \cdot (\text{PF}_6)_4 \cdot (\text{H}_2\text{O})_7$ (C3·4PF<sub>6</sub>·7H<sub>2</sub>O)

To the ligand H<sub>4</sub>L3 (0.245 g, 0.50 mmol), suspended in MeOH (12.5 mL), was added Fe(BF<sub>4</sub>)<sub>2</sub>·6H<sub>2</sub>O (0.337 g, 1.00 mmol) dissolved in MeOH (12.5 mL). After full dissolution, NaPF<sub>6</sub> (0.167 g, 1.00 mmol) and pyridine (2 mL) were added to the maroon-coloured solution. The mixture was stirred for 3 h and filtered, and the filtrate was left to evaporate slowly. X-ray quality crystals were produced after 2 weeks (CCDC 2331489). Found: C, 42.84; H, 4.24; N, 7.92. Calc for C<sub>114</sub>H<sub>131</sub>Fe<sub>7</sub>N<sub>18</sub>O<sub>20</sub>·4PF<sub>6</sub>·7H<sub>2</sub>O: C, 43.19; H, 4.61; N, 7.95.  $\nu_{\text{max}}/\text{cm}^{-1}$  3426(br), 2367, 1617, 1560, 1466, 1300, 1084, 1039, 823, 757, 618, 522, 440.

### 3.3. X-ray Structure Determination

X-ray data of complexes C1 and C2 were recorded at low temperature with a Rigaku-Spider X-ray diffractometer, comprising a Rigaku MM007 microfocus copper rotating-anode generator, high-flux Osmic monochromating and focusing multilayer mirror optics (Cu K<sub>α</sub> radiation,  $\lambda = 1.54178$  Å), and a curved image plate detector. CrystalClear [38] was utilized for data collection and FSProcess in PROCESS-AUTO [39] for cell refinement and data reduction.

Single-crystal diffraction data for C3 were collected at 100 K on the MX2 beamline ( $\lambda = 0.7093$  Å) at the Australian Synchrotron, Victoria, Australia. The dataset was processed and evaluated using XDS [40]. The resulting reflections were scaled using AIMLESS140 from the CCP4 program suite [41]. All structures were solved employing direct methods and expanded by Fourier techniques [42]. All nonhydrogen atoms were refined using anisotropic thermal parameters. The hydrogen atoms were included in the ideal positions with fixed isotropic  $U$  value and were riding on their respective non-hydrogen atoms. Crystal data and refinement parameters for C1–C3 are given in Table A1. CCDC 2331487–2331489 contain the supplementary crystallographic data for this paper.

SQUEEZE results (electrons per formula unit):

C1: Electron count 126

C2: Electron count 232

C3: Electron count 276

### 3.4. Mössbauer Measurements

Samples of 17–29 mg were measured in a custom-made Teflon sample holder. Mössbauer spectra were recorded on a spectrometer from SEE Co. (Science Engineering & Education Co., Edina, MN, USA) equipped with a closed-cycle refrigerator system from Janis Research Co. and SHI (Sumitomo Heavy Industries Ltd., Shinagawa City, Tokyo, Japan). Data were collected in constant acceleration mode in transmission geometry. The zero velocity of the Mössbauer spectra refers to the centroid of the room temperature spectrum of a 25  $\mu\text{m}$  metallic iron foil. Analysis of the spectra was conducted using the WMOSS program (SEE Co, formerly WEB Research Co., Edina, MN, USA).

## 4. Conclusions

The syntheses of one new ‘single-headed’ (**C1**) and two new ‘double-headed’ (**C2** and **C3**) heptanuclear iron complexes formulated as  $[\text{Fe}_3\text{O}-\text{Fe}(\text{OH})_6-\text{Fe}_3\text{O}]$  are reported. Complexes **C2** and **C3** contain a common metallic core,  $[\text{Fe}_7(\mu_3\text{-O})_2(\mu_2\text{-OH})_6]^{+11}$ , which is structurally similar to the  $[\text{Fe}_7(\mu_3\text{-OH})_2(\mu_2\text{-OH})_6]^{+13}$  core of **C1**. The presence of the  $\mu_3\text{-OH}$  groups within the iron triads of **C1** is evidenced by  $^{57}\text{Fe}$  Mössbauer spectroscopy, observed as a significant change to the quadrupole splitting ( $0.50\text{ mm}^{-1}$  and  $0.87\text{ mm}^{-1}$ ) which is consistent with the presence of  $\mu_3\text{-OH}$  groups.

**Supplementary Materials:** The supplementary materials can be downloaded at: <https://www.mdpi.com/article/10.3390/molecules29133218/s1>.

**Author Contributions:** Conceptualization, D.N.T.D.S. and P.G.P.; methodology, D.N.T.D.S.; formal analysis, investigation, and data analysis, T.N.D., D.N.T.D.S., G.B.J., C.G.D., G.N.L.J. and P.G.P.; resources, G.N.L.J. and P.G.P.; writing—original draft preparation, T.N.D. and D.N.T.D.S.; writing—review and editing, T.N.D., G.B.J. and P.G.P.; visualization, T.N.D., C.G.D. and G.N.L.J.; supervision, G.B.J., G.N.L.J. and P.G.P.; project administration, P.G.P.; funding acquisition, P.G.P. All authors have read and agreed to the published version of the manuscript.

**Funding:** This research received no external funding.

**Data Availability Statement:** CCDC 2331487–2331489 contain the supplementary crystallographic data for this paper. These data can be obtained free of charge via [www.ccdc.cam.ac.uk/data\\_request/cif](http://www.ccdc.cam.ac.uk/data_request/cif), or by emailing [data\\_request@ccdc.cam.ac.uk](mailto:data_request@ccdc.cam.ac.uk), or by contacting the Cambridge Crystallographic Data Centre, 12 Union Road, Cambridge CB2 1EZ, UK; fax: +44 1223 336033.

**Acknowledgments:** T.N.D. and P.G.P. would like to thank Massey University for the award of a Massey University Doctoral Scholarship for Māori to T.N.D. The authors would like to thank Heather Jamieson for the collection of synchrotron for complex **C3**.

**Conflicts of Interest:** The authors declare no conflicts of interest.

## Appendix A

**Table A1.** Crystal data and structural refinement parameters for **C1–C3**.

	<b>C1</b>	<b>C2</b>	<b>C3</b>
<b>Formula</b>	$\text{B}_2\text{C}_{162}\text{F}_8\text{Fe}_7\text{H}_{230}\text{N}_{24}\text{O}_{26}$	$\text{B}_4\text{C}_{136}\text{F}_{22}\text{Fe}_7\text{H}_{151}\text{N}_{26}\text{O}_{27}\text{P}$	$\text{C}_{114}\text{H}_{123}\text{Fe}_7\text{N}_{18}\text{O}_{22}$
<b>CCDC</b>	2331487	2331488	2331489
<b>FW (g mol<sup>-1</sup>)</b>	3494.26	3464.98	2488.25
<b>T (K)</b>	153	153	100
<b>Crystal system</b>	trigonal	triclinic	monoclinic
<b>Space group</b>	$R\bar{3}$	$P\bar{1}$	$P2_1/n$
<b>a (Å)</b>	22.558 (5)	17.1685 (11)	15.949 (3)
<b>b (Å)</b>	22.558 (5)	17.3485 (11)	25.627 (5)
<b>c (Å)</b>	33.105 (5)	29.534 (2)	18.611 (4)
<b><math>\alpha</math> (°)</b>	90.000 (5)	86.396 (6)	90
<b><math>\beta</math> (°)</b>	90.000 (5)	76.716 (5)	107.11 (3)
<b><math>\gamma</math> (°)</b>	120.000 (5)	60.913 (4)	90

Table A1. Cont.

	C1	C2	C3
V (Å <sup>3</sup> )	14589 (7)	7469.2 (9)	7270 (3)
Z (Z')	3 (0.167)	2 (1)	2 (0.5)
$\rho_{\text{calc}}$ (g cm <sup>-3</sup> )	1.193	1.541	1.137
$\mu$ (mm <sup>-1</sup> )	4.665	6.32	0.74
F (000)	5526	3560	2582
Crystal size (mm)	0.2 × 0.2 × 0.2	0.33 × 0.23 × 0.21	0.2 × 0.2 × 0.2
Radiation	CuK $\alpha$ ( $\lambda$ = 1.54178)	CuK $\alpha$ ( $\lambda$ = 1.54178)	Synchrotron ( $\lambda$ = 0.71073)
2 $\Theta$ (°)	13.128 to 144.218	13.174 to 130.18	4.302 to 49.426
Index ranges	−27 ≤ h ≤ 26,	−20 ≤ h ≤ 20,	−18 ≤ h ≤ 17,
	−27 ≤ k ≤ 24,	−18 ≤ k ≤ 20,	0 ≤ k ≤ 30,
	−25 ≤ l ≤ 38	−34 ≤ l ≤ 34	0 ≤ l ≤ 21
Reflections collected	43942	96150	43481
Independent reflections	6222 [R <sub>int</sub> = 0.0783, R <sub>sigma</sub> = 0.0531]	24944 [R <sub>int</sub> = 0.1440, R <sub>sigma</sub> = 0.1731]	12205 [R <sub>int</sub> = 0.0487, R <sub>sigma</sub> = 0.0418]
Data/restraints/parameters	6222/78/357	24944/1523/1559	12205/931/861
Goodness-of-fit on F <sup>2</sup>	1.094	1.194	1.079
Final R indexes [I ≥ 2 $\sigma$ (I)]	R <sub>1</sub> = 0.0868, wR <sub>2</sub> = 0.2465	R <sub>1</sub> = 0.1448, wR <sub>2</sub> = 0.4009	R <sub>1</sub> = 0.0784, wR <sub>2</sub> = 0.2466
Final R indexes [all data]	R <sub>1</sub> = 0.0985, wR <sub>2</sub> = 0.2723	R <sub>1</sub> = 0.2433, wR <sub>2</sub> = 0.4638	R <sub>1</sub> = 0.0935, wR <sub>2</sub> = 0.2615
Residual density (e <sup>-</sup> Å <sup>-3</sup> )	1.62/−1.20	0.98/−0.61	0.58/−0.32

## References

- Cohen, I.A. Metal-metal interactions in metalloporphyrins, metalloproteins and metalloenzymes. *Struct. Bond.* **1980**, *40*, 1–37.
- Vincent, J.B.; Olivier-Lilley, G.L.; Averill, B.A. Proteins containing oxo-bridged dinuclear iron centers: A bioinorganic perspective. *Chem. Rev.* **1990**, *90*, 1447–1467. [[CrossRef](#)]
- Horn, A.; Neves, A.; Bortoluzzi, A.J.; Drago, V.; Ortiz, W.A. Crystal structure and magnetic properties of a new tetranuclear iron(III) complex with asymmetric iron coordination as a model for polynuclear iron proteins. *Inorg. Chem. Commun.* **2001**, *4*, 173–176. [[CrossRef](#)]
- Högbom, M.; Nordlund, P. A protein carboxylate coordinated oxo-centered tri-nuclear iron complex with possible implications for ferritin mineralization. *FEBS Lett.* **2004**, *567*, 179–182. [[CrossRef](#)]
- Faiella, M.; Andreozzi, C.; Martin de Rosales, R.T.; Pavone, V.; Maglio, O.; Natri, F.; DeGrado, W.F.; Lombardi, A. An artificial di-iron oxo-protein with phenol oxidase activity. *Nat. Chem. Biol.* **2009**, *5*, 882–884. [[CrossRef](#)] [[PubMed](#)]
- Nogueira, M.L.C.; Pastore, A.J.; Davidson, V.L. Diversity of structures and functions of oxo-bridged non-heme diiron proteins. *Arch. Biochem. Biophys.* **2021**, *705*, 108917.
- Weighardt, K.; Pohl, K.; Jibril, I.; Huttner, G. Hydrolysis products of the monomeric amine complex (C<sub>6</sub>H<sub>15</sub>N<sub>3</sub>)FeCl<sub>3</sub>: The structure of the octameric iron(III) cation of [(C<sub>6</sub>H<sub>15</sub>N<sub>3</sub>)<sub>6</sub>Fe<sub>8</sub>( $\mu_3$ -O)<sub>2</sub>( $\mu_2$ -OH)<sub>12</sub>]Br<sub>7</sub>(H<sub>2</sub>O)]Br·8H<sub>2</sub>O. *Angew. Chem. Int. Ed.* **1984**, *23*, 77–78. [[CrossRef](#)]
- Barra, A.L.; Debrunner, P.; Gatteschi, D.; Schulz, C.E.; Sessoli, R. Superparamagnetic-like behavior in an octanuclear iron cluster. *Europhys. Lett.* **1996**, *35*, 133–138. [[CrossRef](#)]
- Jones, P.L.; Jeffery, J.C.; McCleverty, J.A.; Ward, M.D. Dinuclear and tetranuclear oxo-bridged iron(III) complexes of the ambidentate ligand 3-(2-pyridyl)pyrazole. *Polyhedron* **1997**, *16*, 1567–1571. [[CrossRef](#)]
- Aromi, G.; Brechin, E.K. Synthesis of 3d metallic single-molecule magnets. *Struct. Bond.* **2006**, *122*, 1–67. [[CrossRef](#)]
- Rodriguez, E.; Gich, M.; Roig, A.; Molins, E.; Nedelko, N.; Slawska-Waniewska, A.; Szewczyk, A. Investigations of the stability of [(tacn)<sub>6</sub>Fe<sub>8</sub>( $\mu_3$ -O)<sub>2</sub>( $\mu_2$ -OH)<sub>12</sub>]Br<sub>7</sub>(H<sub>2</sub>O)]Br·8H<sub>2</sub>O (Fe<sub>8</sub>) cluster in aqueous solution by spectroscopic and magnetic methods. *Polyhedron* **2006**, *25*, 113–118. [[CrossRef](#)]
- Boudalis, A.K.; Sanakis, Y.; Raptopoulou, C.P.; Terzis, A.; Tuchagues, J.-P.; Perlepes, S.P. A trinuclear cluster containing the {Fe<sub>3</sub>( $\mu_3$ -O)}<sup>7+</sup> core: Structural, magnetic and spectroscopic (IR, Moessbauer, EPR) studies. *Polyhedron* **2005**, *24*, 1540–1548. [[CrossRef](#)]
- Raptopoulou, C.P.; Sanakis, Y.; Boudalis, A.K.; Psycharis, V. Salicylaldoxime (H<sub>2</sub>salox) in iron(III) carboxylate chemistry: Synthesis, X-ray crystal structure, spectroscopic characterization and magnetic behavior of trinuclear oxo-centered complexes. *Polyhedron* **2005**, *24*, 711–721. [[CrossRef](#)]
- Murray, K.S. Binuclear oxo-bridged iron(III) complexes. *Coord. Chem. Rev.* **1974**, *12*, 1–35. [[CrossRef](#)]
- Shiemke, A.K.; Loehr, T.M.; Sanders-Loehr, J. Resonance Raman study of oxyhemerythrin and hydroxomethemerythrin. Evidence for hydrogen bonding of ligands to the iron-oxygen-iron center. *J. Am. Chem. Soc.* **1986**, *108*, 2437–2443. [[CrossRef](#)] [[PubMed](#)]
- Doi, K.; Antanaitis, B.C.; Aisen, P. The binuclear iron centers of uteroferrin and the purple acid phosphatases. *Struct. Bond.* **1988**, *70*, 1–26.
- Que, L., Jr.; True, A.E. Dinuclear iron- and manganese-oxo sites in biology. *Prog. Inorg. Chem.* **1990**, *38*, 97–200. [[CrossRef](#)]

18. Kurtz, D.M., Jr. Oxo- and hydroxo-bridged diiron complexes: A chemical perspective on a biological unit. *Chem. Rev.* **1990**, *90*, 585–606. [[CrossRef](#)]
19. Nordlund, P.; Sjoeborg, B.M.; Eklund, H. Three-dimensional structure of the free radical protein of ribonucleotide reductase. *Nature* **1990**, *345*, 593–598. [[CrossRef](#)]
20. Holmes, M.A.; Le Trong, I.; Turley, S.; Sieker, L.C.; Stenkamp, R.E. Structures of deoxy and oxy hemerythrin at 2.0 Å resolution. *J. Mol. Biol.* **1991**, *218*, 583–593. [[CrossRef](#)]
21. Wilkins, R.G. Binuclear iron centers in proteins. *Chem. Soc. Rev.* **1992**, *21*, 171–178. [[CrossRef](#)]
22. Solomon, E.I.; Zhang, Y. The electronic structures of active sites in non-heme iron enzymes. *Acc. Chem. Res.* **1992**, *25*, 343–352. [[CrossRef](#)]
23. Mason, K.; Chang, J.; Prescimone, A.; Garlatti, E.; Carretta, S.; Tasker, P.A.; Brechin, E.K. Linking [MIII3] triangles with “double-headed” phenolic oximes. *Dalton Trans.* **2012**, *41*, 8777–8785. [[CrossRef](#)]
24. Thorpe, J.M.; Beddoes, R.L.; Collison, D.; Garner, C.D.; Helliwell, M.; Holmes, J.M.; Tasker, P.A. Surface coordination chemistry: Corrosion inhibition by tetranuclear cluster formation of iron with salicylaldoxime. *Angew. Chem. Int. Ed.* **1999**, *38*, 1119–1121. [[CrossRef](#)]
25. Gass, I.A.; Milios, C.J.; Collins, A.; White, F.J.; Budd, L.; Parsons, S.; Murrie, M.; Perlepes, S.P.; Brechin, E.K. Polymetallic clusters of iron(III) with derivatized salicylaldoximes. *Dalton Trans.* **2008**, 2043–2053. [[CrossRef](#)] [[PubMed](#)]
26. Mason, K.; Gass, I.A.; Parsons, S.; Collins, A.; White, F.J.; Slawin, A.M.Z.; Brechin, E.K.; Tasker, P.A. Building Fe(III) clusters with derivatised salicylaldoximes. *Dalton Trans.* **2010**, *39*, 2727–2734. [[CrossRef](#)] [[PubMed](#)]
27. Mason, K.; Chang, J.; Garlatti, E.; Prescimone, A.; Yoshii, S.; Nojiri, H.; Schnack, J.; Tasker, P.A.; Carretta, S.; Brechin, E.K. Linking [Fe<sup>III</sup><sub>3</sub>] triangles with “double-headed” phenolic oximes. *Chem. Commun.* **2011**, *47*, 6018–6020. [[CrossRef](#)] [[PubMed](#)]
28. Holynska, M.; Clerac, R.; Langer, T.; Poettgen, R.; Dehnen, S. Selective syntheses, structures and magnetic properties of Fe(III) complexes of different nuclearities. *Polyhedron* **2013**, *52*, 1425–1430. [[CrossRef](#)]
29. Wenzel, M.; Forgan, R.S.; Faure, A.; Mason, K.; Tasker, P.A.; Piligkos, S.; Brechin, E.K.; Plieger, P.G. A New Polynuclear Coordination Type for (Salicylaldoxime)copper(II) Complexes: Structure and Magnetic Properties of an (Oxime)Cu<sub>6</sub> Cluster. *Eur. J. Inorg. Chem.* **2009**, *2009*, 4613–4617. [[CrossRef](#)]
30. De Silva, D.N.T.; Dais, T.N.; Jameson, G.B.; Cutler, D.J.; Brechin, E.K.; Davies, C.G.; Jameson, G.N.L.; Plieger, P.G. Synthesis and Characterization of Symmetrically versus Unsymmetrically Proton-Bridged Hexa-Iron Clusters. *ACS Omega* **2021**, *6*, 16661–16669. [[CrossRef](#)]
31. Aldred, R.; Johnston, R.; Levin, D.; Neilan, J. Magnesium-mediated ortho-specific formylation and formaldoximation of phenols. *J. Chem. Soc. Perkin Trans.* **1994**, *1*, 1823–1831. [[CrossRef](#)]
32. Stevens, J.R.; Plieger, P.G. Anion-driven conformation control and enhanced sulfate binding utilising aryl linked salicylaldoxime dicopper helicates. *Dalton Trans.* **2011**, *40*, 12235–12241. [[CrossRef](#)] [[PubMed](#)]
33. Forgan, R.S.; Davidson, J.E.; Galbraith, S.G.; Henderson, D.K.; Parsons, S.; Tasker, P.A.; White, F.J. Transport of metal salts by zwitterionic ligands; simple but highly efficient salicylaldoxime extractants. *Chem. Commun.* **2008**, 4049–4051. [[CrossRef](#)] [[PubMed](#)]
34. Steiner, T. Reviews: The hydrogen bond in the solid state. *Angew. Chem. Int. Ed.* **2002**, *41*, 48–76. [[CrossRef](#)]
35. *Mössbauer Spectroscopy of Environmental Materials and Their Industrial Utilization*; Murad, E.; Cashion, J. (Eds.) Springer: New York, NY, USA, 2004; p. 440.
36. Wang, Q.; Wilson, C.; Blake, A.J.; Collinson, S.R.; Tasker, P.A.; Schroeder, M. The one-pot halomethylation of 5-substituted salicylaldehydes as convenient precursors for the preparation of heteroditopic ligands for the binding of metal salts. *Tetrahedron Lett.* **2006**, *47*, 8983–8987. [[CrossRef](#)]
37. Plieger, P.G.; Tasker, P.A.; Galbraith, S.G. Zwitterionic macrocyclic metal sulfate extractants containing 3-dialkylaminomethylsalicylaldimine units. *Dalton Trans.* **2004**, 313–318. [[CrossRef](#)]
38. *CrystalClear*; 1.4.0; Rigaku Americas Corporation: The Woodlands, TX, USA, 2005.
39. *PROCESS-AUTO*; Rigaku Corporation: Tokyo, Japan, 1998.
40. Kabsch, W. XDS. *Acta Crystallogr. Sect. D* **2010**, *66*, 125–132. [[CrossRef](#)] [[PubMed](#)]
41. Winn, M.D.; Ballard, C.C.; Cowtan, K.D.; Dodson, E.J.; Emsley, P.; Evans, P.R.; Keegan, R.M.; Krissinel, E.B.; Leslie, A.G.W.; McCoy, A.; et al. Overview of the CCP4 suite and current developments. *Acta Crystallogr. Sect. D* **2011**, *67*, 235–242. [[CrossRef](#)]
42. Sheldrick, G.M. A short history of SHELX. *Acta Crystallogr. Sect. A Found. Crystallogr.* **2008**, *64*, 112–122. [[CrossRef](#)]

**Disclaimer/Publisher’s Note:** The statements, opinions and data contained in all publications are solely those of the individual author(s) and contributor(s) and not of MDPI and/or the editor(s). MDPI and/or the editor(s) disclaim responsibility for any injury to people or property resulting from any ideas, methods, instructions or products referred to in the content.